Numerical and experimental investigation of asymmetrical contact between a steel plate and armour-piercing projectiles

Piotr Pawlowski[1], Teresa Fras[2]

[1]Institute of Fundamental Technological Research Polish Academy of Sciences (IPPT PAN), Warsaw, Poland
[2]French-German Research Institute of Saint-Louis (ISL), Saint-Louis, France

1 Introduction

Protection of combat-vehicles against impacts of small-calibre projectiles may be improved by the application of relatively thin and hard steel plates perforated by a plurality of holes. It is observed that due to the contact with a plate, the core of armour-piercing (AP) projectiles may be shattered, partially eroded or rotated, depending on the hit-position. The contact asymmetry is the strongest when a projectile hits a hole edge, its core undergoes bending and tends to fracture. The presented study discusses two methods of modelling of the contact and interactions between a bullet and a steel target. One of them is the explicit Lagrangian simulation of impacts of a fully represented AP projectile, another one is the semi-analytical model based on the integration of the motion equations of a 6 DOF rigid projectile. The results of numerical and semi-analytical approaches are compared with the ballistic impact experiment, in which the defeat mechanisms provided by 4-mm-thick slotted bainitic plates (Pavise™ SBS 600P) against hard-core 7.62 mm P80 0.30 AP x 51 (.308 Win) projectiles were verified, [1].

2 Ballistic impact tests

Ultra high-hardness perforated armour steel Pavise™ SBS 600P belongs to a group of so called 'super-bainitic' steels, which due to its refined nano-structure are very strong and relatively ductile, [2-5]. The steel has an ultimate tensile strength of 2500 MPa, hardness at 600 - 670 HV and toughness in excess of 30 - 40 $MPam^{1/2}$, [5]. A combination of the ultra-fine nano-scale structure coupled with the specially designed pattern of perforations results in an efficient perforated steel armour. In the study, 4-mm-thick plates slotted by elongated holes (4 x 12 mm) were tested against 7.62 x 51 AP P80 projectiles, which according to the requirement of VPAM [6] (the standardized procedure of evaluating a protection level for logistic- and light-armoured vehicles) cannot perforate a tested armour at an impact velocity of 820 +/- 10 m/s. The AP projectile is composed of the brass jacket, hardened steel core, lead-antimony cap. It weights 24 g, the core of hardness 62 +/- 2 HRC has mass of 4 +/- 0.1 g, [7].
During the experiment, over 20 shots were performed. Shots were categorized in three general groups according to a hit point and the resulted projectile failure (details in [1]). It was observed that an AP projectile may be strongly rotated if it goes through a hole, its core may be broken in its half if a projectiles hits a hole-edge or, if it hits the area between holes, the core tip erodes and the remaining core is strongly deviated from its initial trajectory. Two examples of core deviation resulted from the asymmetric contact between the bullet and the perforated plate are shown in Fig. 1. In the first case, the projectile hits in a hole; in the second, the bullet perforates the material between holes. The flash X-ray device was used to record the trajectory of the distorted core, providing exposure of the projectile in three time instances. The first X-ray image was taken just before the impact; the second and the third images captured the projectile at the distance 50 and 130 mm behind the plate. The position of the projectile tip in the moment of impact was recorded by an ultra-high speed camera. When a projectile hits inside a hole, its tip passes through it without damage but the projectile periphery touches the inner edges of the hole, which leads the undamaged core to obtain a high rotation. In the discussed case, after 130 mm of flight, the core was almost parallel to the plate (the spatial angle of the core was found to be equal to 83°). The initial impact velocity of the bullet was measured as 826 m/s; after passing through the pre-armour plate the velocity was reduced to 714 m/s.

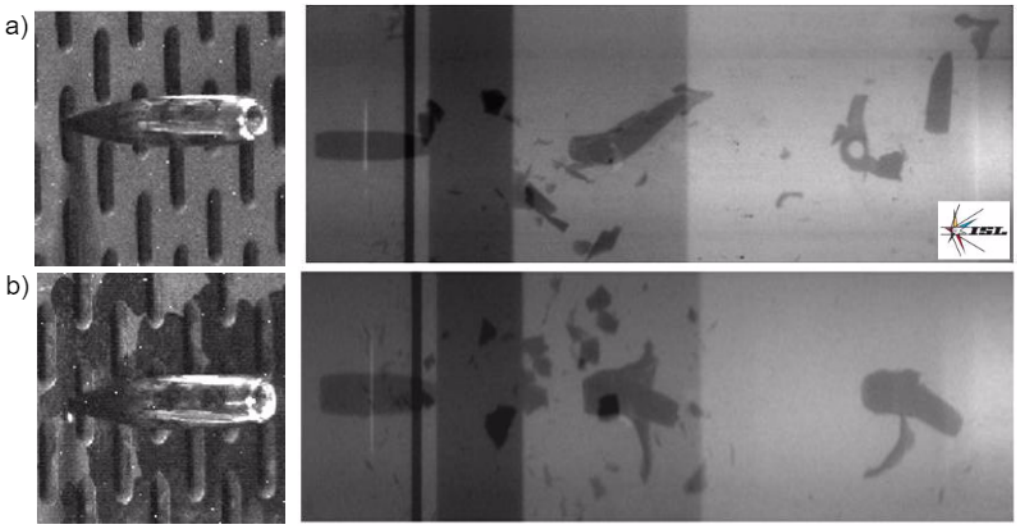

Fig.1: The high speed camera and flash X-ray images of the projectile which hit: a) in a hole and b) in the material.

In the case when a projectile hits the material between holes, its core was only partly eroded due to the contact with the plate. The rotation of the core, more distinct after 130 mm of its flight, was measured as 32°. The bullet velocity decreased from 825 m/s to 753 m/s.

3 Numerical modelling of ballistic impacts

The numerical simulation aimed to show significant differences between impacts into different points of perforated plates. A numerical model of high-velocity impacts should represent a nonlinear behaviour of interacting materials, their large deformation and final fragmentation. The functions and boundary conditions used in calculations must allow the material failure to be properly modelled.

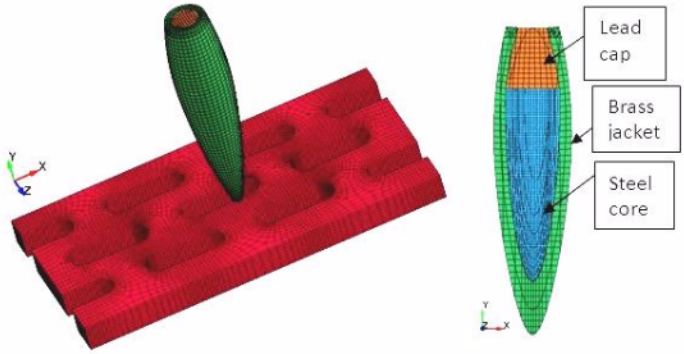

Fig.2: Numerical representation of the impact configuration.

In the calculations, the material model parameters of the target's and the bullet's parts were taken from works [8-9] (see [1]). The popular phenomenological functions dependent on strain, temperature and strain rate are applied to describe the materials, i.e. the Johnson-Cook flow and fracture models, [10-11]. The constitutive relation coupled with the function describing fracture is implemented in LS-DYNA as *MAT_MODIFIED_JOHNSON_COOK (*MAT_107), [12]. In order to allow a crack growth during the penetration process, the model is coupled with a damage evolution rule – details may be found in the Ls-Dyna manual [13] and papers of Børvik, e.g. [12]. The core is modelled using *MAT_SIMPLIFIED_JOHNSON_COOK (*MAT_98). The JC flow model does not account for effects of temperature on the material deformation. Failure of core elements is possible due to the option *MAT_ADD_EROSION coupled with the flow model. To obtain a core fracture two erosion thresholds are applied, which may be treated as an artificial model of material fracture. MNPRES (minimum pressure at failure) and EPSH (shear strain at failure) cause the element erosion if the assumed value

of pressure or shear strain is reached. The plates are fully clamped and the initial velocity is applied to the projectile. The contact between the plates and the projectile and between projectile parts is modelled using an eroding algorithm *ERODING_SURFACE_TO_SURFACE. Friction between parts is not considered. The plates and projectile are meshed regularly by 8-node constant-stress solid elements with one integration point and stiffness-based hourglass control. All parts of the AP projectile (brass jacket, lead filler and bullet core) are included in the numerical model, Fig. 2. A mesh of element size 0.4 x 0.4 x 0.4 mm is assumed for the plate, the mesh size of the core is 0.2 x 0.2 x 0.2 mm.

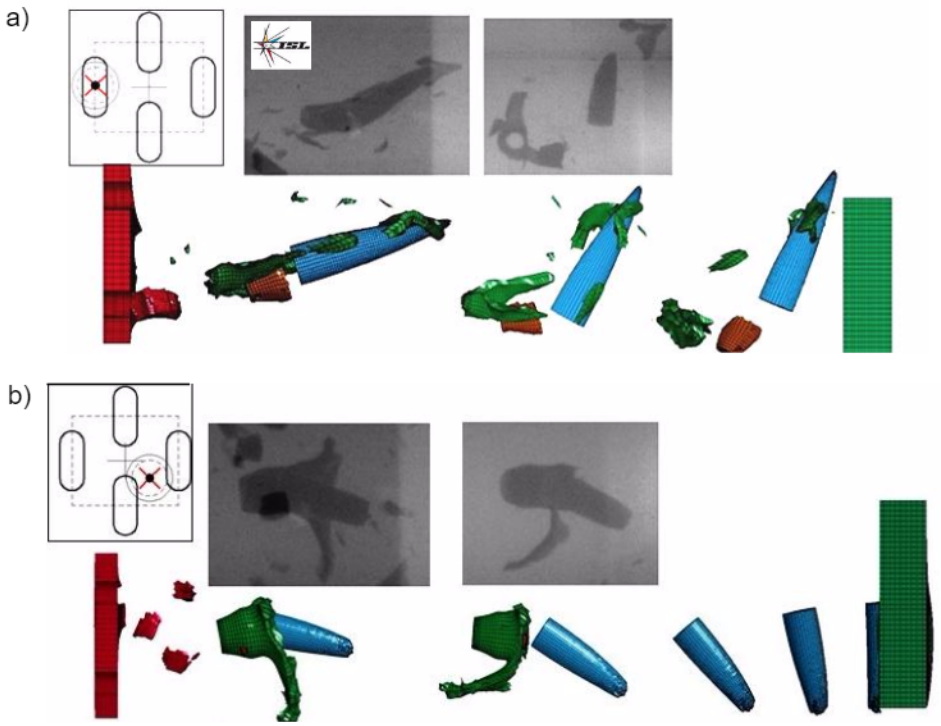

Fig.3: Numerical results of the AP impact in: a) a hole and b) an area between holes compared with the flash X-ray images.

The results of the simulation of impact inside a hole are presented in Fig.3a. Since the projectile diameter is slightly wider than the hole-width, when it hits in a hole, the brass jacket is fully peeled off and the core is deviated due to the contact with the inner hole-surfaces. In the case when the projectile perforates the bulk material of the plate (Fig.3b), even slight asymmetric interactions cause a partial erosion of its tip and introduce the core rotation. Contact forces and a change of geometrical properties of the bullet disturb its initial trajectory and reduce the initial velocity.

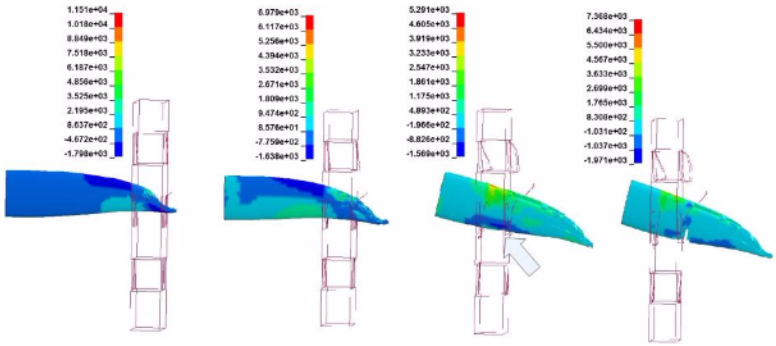

Fig.4: Core undergoes bending induced by the contact with a hole edge (maps of pressure [MPa] in time, the erosion condition for the core: MNPRES = -2000 MPa).

The protective effectiveness of perforated armours is mostly dependent on asymmetric contact interactions causing a large distortion of projectile's trajectory combined with heavy bending of its core. The steel of core is characterised by high strength, hardness and low ductility, which result in a low core susceptibility to bending leading to fracture, Fig. 4. Impacts in hole edges result in a core fragmentation and should be considered as the most efficient case of reducing perforating properties of small-calibre projectiles. As the initial yaw and pitch angles of projectiles are equal to zero and the axis of impact are perpendicular to the plate having no influence on the final trajectory (see Fig.1), the final deviation of cores results from the contact asymmetry between the projectile and the plate.

4 Simplified semi-analytical modelling of asymmetric contacts

The explicit finite-element modelling of interactions between the plate and projectile provides good qualitative and quantitative results in comparison to the experimental ones. The numerical approach has however several disadvantages resulting in high computational costs, like a necessity of a proper mechanical characterisation of hardening and fracture of interacting materials or a large number of elements required for reliable modelling of crack propagations. These issues become even more pronounced in case of topological optimization of slotted amours, which requires extensive numerical computations of objective functions for different spatial patterns of perforation holes.
In order to improve the modelling effectiveness, the authors propose a 3D semi-analytical model based on the integration of the equations of motion of a 6 DOF rigid projectile. In such a robust model, the projectile-plate interactions are simplified and based on the integration of stress components, which are normal and tangent to the projectile's contact surface. Simplified analytical and semi-analytical models are often applied in the problems related to terminal ballistics, [14]. The presented approach belongs to a group of local interaction models, which are widely discussed in [15], and successfully applied for edge-impact simulations in e.g. [16]. The model is implemented in the software for mathematical computations Matlab and compared with experimental and numerical results obtained in Ls-Dyna.
The discussed semi-analytical model is based on several simplifications of physical phenomena occurring between bodies in contact, which seem to be justified in case of impact of ogive projectiles into thin metallic plates, in which the target deformation is dominated by plastic flow. Because the mechanical strength of the core and plate are higher than those of the jacket and lead, the projectile is modelled only as its rigid core with 6 degrees of freedom, with its surface discretized by a regular grid of points. Due to its rotational symmetry the AP projectile's geometry is modelled as an analytical surface of revolution obtained by rotation of a second order polynomial curve of the form $y(x) = a_2 x^2 + a_1 x + a_0$, with $x = 0$ located in the centre of gravity and coefficients $a_2 = -5.29$; $a_1 = 0.24$; $a_0 = 0.0003$, which were fitted to the geometry of the numerical Lagrangian model. The analytical description of the surface allows for using analytical formulae for the normal and tangent vectors (**n**, **t**), which are necessary to calculate the contact forces.
The formulation and time integration of equations of motion follow the classical approach for the 6 DOF rigid body motion, which can be found in classical texts on flight dynamics, e.g. [17-19]. The first differential equation for the translational movement is based on the Newton's second law referenced to the global inertial frame, applied to the point mass m located in the centre of mass of the projectile.

$$\mathrm{m}\,\ddot{\mathbf{x}} = \mathbf{F}_\mathrm{I} \tag{1}$$

The rotational position and angular velocities of the projectile in the inertial reference system are described by the three Euler angles $\boldsymbol{\Theta}$ (yaw, pitch and roll) and their rates. Because the equations of motion have much simpler forms in the body coordinate system, which rotates with the rigid projectile, the angle rates $\boldsymbol{\omega}$ are represented in the body frame as follows:

$$\dot{\boldsymbol{\omega}} = \begin{bmatrix} \mathrm{p} \\ \mathrm{q} \\ \mathrm{r} \end{bmatrix} = \begin{bmatrix} 1 & 0 & -\sin\theta \\ 0 & \cos\varphi & \cos\theta\sin\varphi \\ 0 & -\sin\varphi & \cos\theta\cos\varphi \end{bmatrix} \begin{bmatrix} \dot{\varphi} \\ \dot{\theta} \\ \dot{\psi} \end{bmatrix} \quad \text{and} \quad \dot{\boldsymbol{\Theta}} = \begin{bmatrix} 1 & \sin\varphi\tan\theta & \cos\varphi\tan\theta \\ 0 & \cos\varphi & -\sin\varphi \\ 0 & \sin\varphi\sec\theta & \cos\varphi\sec\theta \end{bmatrix} \begin{bmatrix} \mathrm{p} \\ \mathrm{q} \\ \mathrm{r} \end{bmatrix} \tag{2}$$

In the body coordinate system, the tensor of inertia **I** is constant and moreover, if the projectile is rotationally symmetrical the axes of the body coordinate system of the projectile are the principal axes of **I**. The conservation of the angular momentum **H** in the local, moving system can be now expressed as:

$$\dot{\mathbf{H}} = \mathbf{M}, \quad \text{where} \quad \dot{\mathbf{H}} = \begin{bmatrix} I_{xx}\dot{p} + (I_{zz} - I_{yy})qr \\ I_{yy}\dot{q} + (I_{xx} - I_{zz})pr \\ I_{zz}\dot{r} + (I_{yy} - I_{zz})pq \end{bmatrix}, \quad \mathbf{M} = \begin{bmatrix} M_x \\ M_y \\ M_z \end{bmatrix}, \tag{3}$$

The vectors of resultant force **F** and moment **M** can be calculated as a sum of point forces $\mathbf{F}_i$ and their moments about the centre of mass of the projectile's core in its current configuration:

$$\mathbf{F} = \sum_i \mathbf{F}_i \,, \quad \mathbf{M} = \sum_i \mathbf{r}_i \times \mathbf{F}_i \tag{4}$$

Force vector **F** before using in the eq. 1 must be transformed to the global inertial reference frame from the current rotated body coordinate system of the projectile. An example of resultant force and moment vectors in the projectile's reference frame is presented in Fig. 5b, while Fig. 5a presents a field of unit normal vectors at points discretizing the surface of the core.

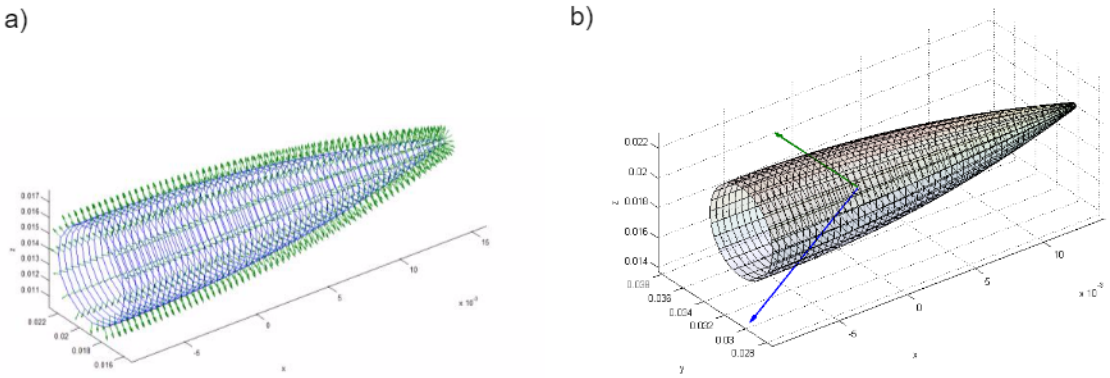

Fig.5: View of the surface of the AP projectile with a) plotted field of unit normal vectors, b) resultant force (blue) and moment (green) vectors acting on the rigid projectile.

The geometry of the target perforated plate is modelled as *i x j* matrix (*i = H/dx*, *j =L/dx*, where *H* and *L* are the total height and width of the plate and *dx* is the distance between points) representing regular grid of points. This means that an element of the matrix (i, j) is related to a discrete geometrical point (y_i, z_j) of the target. Each element of the matrix contains a value describing the phenomenological material resistance *Y*, c.f. Fig. 6.

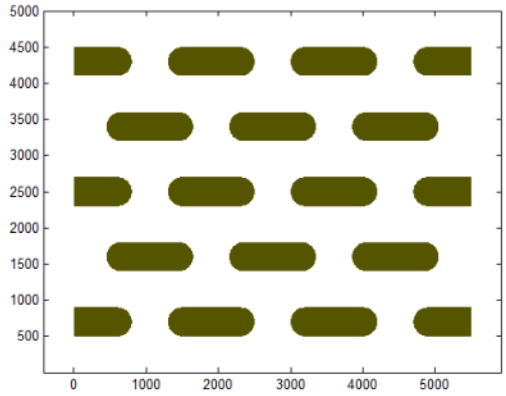

Fig.6: View of the matrix representing the perforated terget plate with elongated holes, Y = 0 in the area of holes.

The contact forces between the projectile and the plate are calculated at each point of the projectile grid. At each time step, a set of projectile's points inside the target is calculated. Each point is

projected to its nearest neighbour at the target and the local contact force vector is computed according to the formula (5).

$$\mathbf{F}_i = \begin{cases} Y(x_i, y_i)(\mathbf{n}_i + \eta \mathbf{t}_i) dS_i & if\ Y(x_i, y_i) > 0 \\ \mathbf{0} & otherwise \end{cases} \quad (5)$$

The non-dimensional coefficient η represents shear or friction resistance of the target in the tangent direction and dS_i is the surface area related to each point of the core.
Values of the target resistance Y at points subjected to contact with the projectile are subjected during analysis to algorithm of degradation:

$$Y(x_i, y_i)_{t+1} = \beta\, Y(x_i, y_i)_t \text{ , where } \beta \in \langle 0,1 \rangle \quad (6)$$

The relation (6) presents the most simplified, linear form of local interaction equation, which can be expressed in the most general formulation as a nonlinear function of normal and tangent vector and interface velocities [15].

5 Comparison with experimental results

The two experimental tests presented in the paragraphs 2 and 3 were re-calculated using the simplified model discussed above. At this point of research, the parameters of the model were not identified by any optimisation algorithm or experimental procedure. The values of Y, η and β were assumed as: 2600 x 10^6 Pa, 0.05 and 0.8, respectively. The target was discretized by a grid of points with spacing of 1^{-5} m. The surface of the projectile was divided into 1296 points.

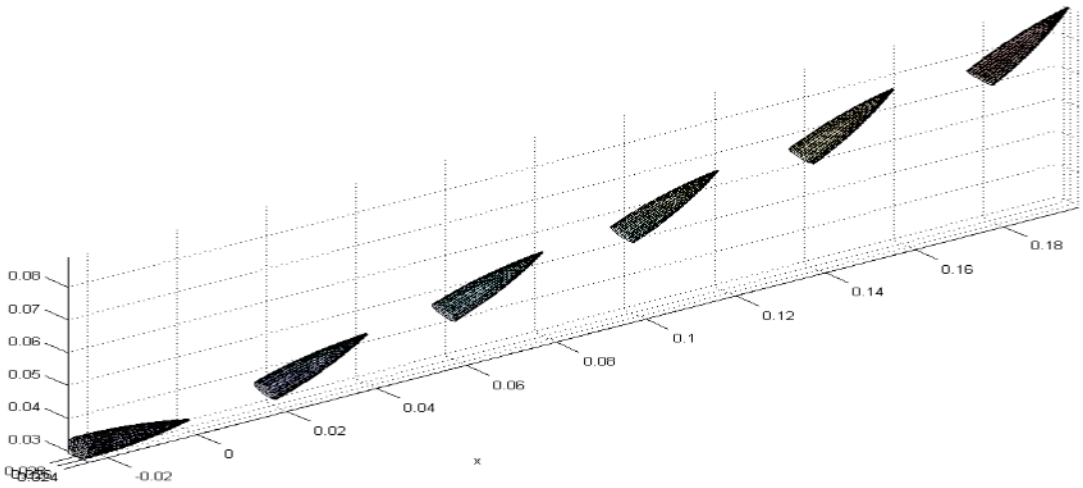

Fig.7: Views of selected time instances of the position and rotation of the AP projectile which passes through a hole.

In the first case representing the impact inside a hole, the initial velocity was reduced from 825 m/s to 746 m/s. The results of the experiment, of the numerical simulation in Ls-Dyna and those obtained due to the simplified model are compared in the Table1.

	residual velocity [m/s]	pitch@50mm [deg]	yaw @50mm [deg]	pitch@130mm [deg]	yaw@130mm [deg]
experiment	714	24	4	83	64
Ls-Dyna model	714	15	0	61	6
simplified model	746	21	0	22	0

Table 1: Comparison of the numerical and experimental results for the impact inside a hole.

It can be noted that the simplified model underestimates the residual velocity by approximately 5% and rotating moments obtained during the contact with the target result in angular rates, which cannot provide the right pitch angle. The trajectory of the projectile is presented in Fig. 7, whereas in Fig. 8, there are compared the pitch and yaw angles of the projectile for time instances representing distance just before the beginning of penetration and 50 and 130 mm after the target penetration. The experimental images are not perfectly aligned and scaled; therefore, this comparison should be regarded only as indicative.

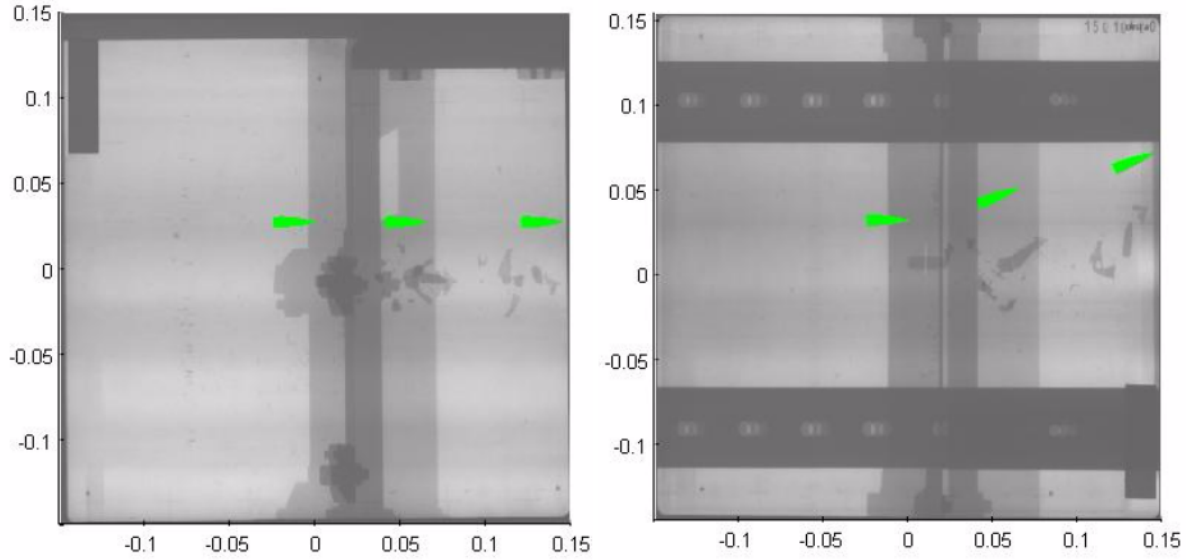

Fig.8: Comparison of projectile trajectiories in three time instances – before the impact, at 50 and 130 mm from the perforated plate: a) XY view (yaw angle), b) XZ view (pitch angle).

The analogical comparison of results for the impact between holes is presented in Table 2. The initial velocity was reduced from 825 m/s to 730 m/s, which is much closer to the experimental value of 753 m/s than in the first case. The pitch angle after 50 mm has much lower value from the experimental result; however, this discrepancy diminishes at 130 mm. The graphical representation of projectiles trajectory was depicted in Figs. 9-10.

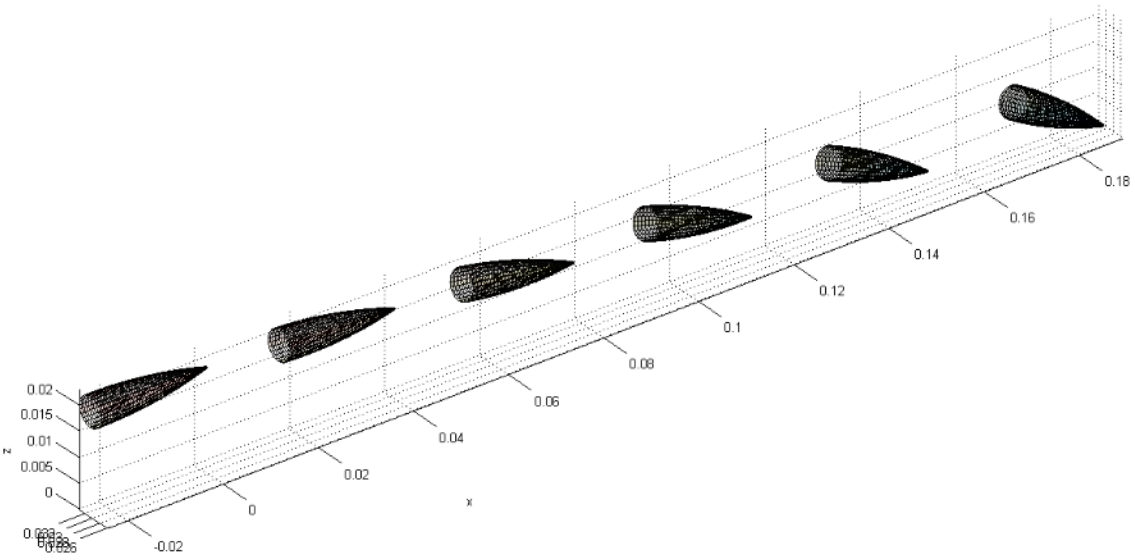

Fig.9: Views of selected time instances of the position and rotation of the AP projectile, which hits the material between holes.

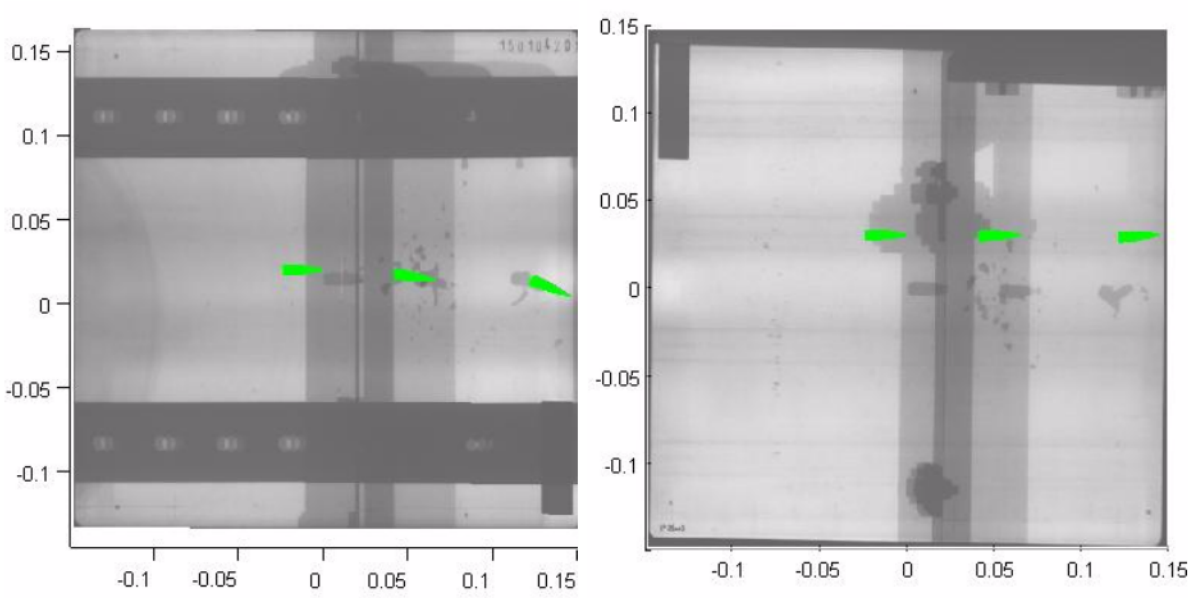

Fig.10: Comparison of projectile trajectiories in three time instances – before the impact, at 50 and 130 mm from the perforated plate: a) XY view (yaw angle), b) XZ view (pitch angle).

It was experimentally proven that perforated plates are efficient add-on passive armours in application against impacts of small calibres. It is already known that the size of holes and plate thickness must be adjusted to a threat but the most efficient hole pattern is still not known. Steel manufacturers offer plates which are made with steels of diverse properties, of different thicknesses and several holes patterns (elongated, circular or even triangular, [20-21]). Although the quantitative results obtained from the simplified model show moderate accuracy in representing the very complex behaviour of the projectile-target system, they closely follow the tendency of changes of trajectories for the two considered different impact conditions. The model will be further developed and validated on more extensive range of experimental scenarios and numerical test cases generated in Ls-Dyna. It also requires a new methodology for correct estimation of material parameters of the model, based e.g. on ballistic test curve results.

	residual velocity [m/s]	pitch@50mm [deg]	yaw @50mm [deg]	pitch@130mm [deg]	yaw@130mm [deg]
experiment	753	16	1	23	25
Ls-Dyna model	790	16	0	35	4
simplified model	730	8.5	1	23	4

Table 2: Comparison of the numerical and experimental results for the impact in the area between holes.

To conclude, the presented semi-analytical model may be applied as a simplified method for the efficient evaluation of different geometries of perforated plates and in consequence, as a tool for their topological optimization.

6 Summary

4 mm thick bainitic plate perforated by slotted holes reduces significantly impact energy of 7.62 x 51 (.308 Win) hard-core AP projectiles, which due to the contact with the plate may be broken or distracted. Basing on the performed ballistic experiment, the discussion on modelling of interactions AP projectiles and add-on perforated plates is realized by the explicit FEM simulation and the simplified modelling based on the integration of the equations of motion of a rigid projectile.

The numerical simulation was performed in Lagrangian approach, in which plastic hardening, fracture of elements of the projectile and plate were modelled by the *MAT_107, the contact was assumed as *ERODING_SURFACE_TO_SURFACE which allowed for the element erosion. The numerical modelling of impacts confirmed dependence between the projectile failure and the hit point.
The simplified, localized-interaction model based on the integration of the equations of motion of a 6 DOF rigid projectile proved also its efficiency in predicting the core behaviour in dependence on the hit position. The semi-analytical model provided results in the computation time much shorter than the explicit calculations. In such a robust model, the projectile-plate interactions are simplified and based on the integration of stress components, which are normal and tangent to the projectile's contact surface. In particular, the model might be applied as a simplified method of the topological optimisation of the geometry of perforated plates.

7 Literature

[1] Fras T, Murzyn A, Pawlowski P. "Defeat mechanisms provided by slotted add-on bainitic plates against allcalibre 7.62 mm x 51 AP projectiles". Int J Impact Eng 103, 2017,241-53.
[2] http://www.army-technology.com/features/featuresuper-bainite-steel-perfection-in-impenetrability-4346392/ (2016)
[3] http://www.cam.ac.uk/research/features/steels-inner-strength (2016)
[4] Bhadeshia HKDH. "Bainite in steels". Inst. of Metals,1992,1-8.
[5] Caballero FG, Bhadeshia HKDH. "Very strong bainite". Current Opinion in Solid State and Materials Science 8, 2004, 251–7.
[6] VPAM APR 2006. "General basis for ballistic material, construction and product tests - Requirements, test levels and test procedures". Ed. 2009.
[7] http://www.men-defencetec.de/en/produkte/militaer/762-mm-x-51-308-win/detailview/?tx_men_pi1%5Bproduktlinie%5D=2&tx_men_pi1%5Bkaliber%5D=1&tx_men_pi1%5Bdetail%5D=5&cHash=6618e9d6e6fa469d9e670b47c77b5bdd (2016)
[8] Wisniewski A, Żochowski P. "A constitutive model for the nanocomposite NANOS-BA steel used for light armored vehicles protection". Proceed 27th Int Symp on Ballist Freiburg 2013.
[9] Børvik T, Dey S, Clausen AH. "Perforation resistance of five different high strength steel plates subjected to small-arms projectiles". Int J Impact Eng 36, 2009, 948–64.
[10] Johnson GR, Cook WH. "Fracture characteristics of three metals subjected to various strains, strain rates, temperatures and pressures". Eng Fract Mech 21,1985,31–48.
[11] Johnson GR, Cook WH. "A constitutive model and data for metals subjected to large strains, high strain rates and high temperatures". Proceed 7th Int Symp on Ballistics the Hague 1983.
[12] Børvik T, Hopperstad OS, Berstad T, Langseth M. "A computational model of viscoplasticity and ductile damage for impact and penetration". Eur J Mech A/Solids 20(5), 2001, 685–712.
[13] LS-DYNA Support. Manual, http://www.dynasupport.com/news/ls-dyna-971-manual-pdf (2016)
[14] Rosenberg Z, Dekel E, "Terminal Ballistics", Springer, 2012
[15] Ben-Dor G, Dubinsky A, Elperin T. "Ballistic Impact: Recent Advances in Analytical Modeling of Plate Penetration Dynamics-A Review". Appl Mech Rev 58.6, 2005, 355–71.
[16] Mayseless M, Cooper Z, Reifen A, Yaziv D. "Deflecting and rotating rigid projectile hitting plate edge", Proceed 27th Int Symp on Ballist Miami 2011.
[17] Stengel R.F. "Flight Dynamics", Princeton University Press, 2004.
[18] Stengel R.F. "Lecture Slides for Aircraft Flight Dynamics, MAE 331, Fall 2016", online: http://www.princeton.edu/~stengel/MAE331Lectures.html
[19] Jenkins PN. "Technical Report Rg-Pa-17 Missile Dynamics Equations for Guidance and Control Modeling and Analysis", Guidance and Control Directorate, US Army Missile Laboratory, APRIL 1984.
[20] Auyer RA, Buccellato RJ, Petrick EN, Sridharan NS. "Armor plate having triangular holes". Patent No: US 4835033; 1989.
[21] Radisavljevic I, Balos S, Nikacevic M, Sidjanin L. "Optimization of geometrical characteristics of perforated plates". J Mater & Des 49, 2013,81–9.